

## Self-focusing of an optical beam in a plasma

T. Kurki-Suonio, P. J. Morrison, and T. Tajima

*Department of Physics and Institute for Fusion Studies, The University of Texas at Austin, Austin, Texas 78712*

(Received 21 March 1989)

Self-focusing of an intense optical beam in a plasma is studied, including the nonlinear effects of both the relativistic electron mass and the ponderomotive potential due to the electromagnetic wave. An exact steady-state asymptotic solution of beam propagation in a localized solitary waveform is obtained in slab geometry. Amplitude-width scaling relations are obtained, which imply that the width is limited to be less than the square root of three collisionless skin depths. In the weakly relativistic limit our solution reduces to the solution obtained by Schmidt and Horton [Comm. Plasma Phys. Controlled Fusion E 9, 85 (1985)]. Solutions where the beam profile is of oscillatory nature, which correspond to the presence of the steady-state solution of a multiple-beamlet profile, are also presented. Finally, the asymptotic nature of the solitary wave is tested using a recently developed numerical particle simulation code.

### I. INTRODUCTION

The nonlinear self-focusing of intense electromagnetic radiation in a dielectric medium has been studied for well over 20 years.<sup>1</sup> The development of powerful lasers and their various applications has prompted a considerable interest in self-focusing processes in plasma. In particular, the concepts of laser-ignited fusion and laser-plasma particle accelerators such as the beat-wave accelerator<sup>2</sup> and the plasma-fiber accelerator,<sup>3</sup> require transport of the laser beam with minimal loss in intensity over a considerable distance. A mechanism that allows for such a transport of the beam, without significant depletion, is discussed here.

Optical communication via laser pulses is another area in which transport of an optical beam has been considered. Hasegawa *et al.*<sup>4,5</sup> have considered shaping of laser pulses into a soliton in order to increase the packing density of information and to reduce loss. Mima *et al.*<sup>6</sup> considered a triple soliton profile of a laser pulse to avoid the laser-pulse depletion in a plasma. These methods rely on shaping the longitudinal profile of optical beams. In the present paper, however, we focus our discussion on the transverse profile of optical beams in a plasma.

As an intense laser beam enters plasma, an initial transient phase is expected. The interesting question is, what kind of a stationary state will the system assume after the initial transient. In particular, what is the asymptotic or steady form of the beam profile as it traverses through the plasma. Solitonlike or solitary-wave profiles (either single or multiple) have emerged from several studies. An asymptotic profile of solitary nature would indeed be welcome for the above-mentioned applications<sup>1-3</sup> (particularly for the plasma-fiber accelerator<sup>3</sup>) because for such a profile the beam propagates without transverse spreading and thus, without losing its intensity or profile in this way.

In this paper we obtain asymptotic profiles for short laser pulses propagating in a cool plasma. The advantage

of using a short laser pulse is that the ions, being massive, do not have time to respond and thus can be taken to be immobile. Therefore the laser-plasma system should be free of the parametric instabilities associated with the ion motion. The self-focusing process for a quasineutral plasma<sup>7</sup> is absent due to the short time scale. Since we are studying a cool plasma, only ponderomotive and relativistic effects are considered: the thermal self-focusing<sup>8</sup> effect should be negligible.

In Sec. II we present the basic evolution equations for the laser-plasma system. In Sec. III we look for an asymptotic profile of the laser beam by taking an ansatz which makes the evolution equations separable. The equations are solved analytically in slab approximation. Comparisons to earlier work on the subject are made. In Sec. IV the asymptotic profile obtained analytically is tested using a particle simulation program. In Sec. V the results derived are summarized.

### II. EVOLUTION EQUATIONS FOR LASER INTENSITY PROFILE

The basic set of equations describing the laser-plasma system consists of Maxwell's equations and the equation of motion for relativistic electrons. The electron pressure gradient is neglected in comparison with the ponderomotive force and the electrons are treated as cold. The assumption of immobile ions, justified as previously mentioned by the shortness of the laser pulse, allows us to write the charge density and plasma current in terms of the equilibrium density  $n_0$  and the electron density perturbation  $\delta n_e$ :

$$\begin{aligned} \sum_j e_j n_j &= -e \delta n_e, \\ \mathbf{J} &= -e(n_0 + \delta n_e) \mathbf{v}. \end{aligned} \quad (1)$$

Expressing the electromagnetic fields in terms of the potentials we obtain

$$\frac{\partial^2 \mathbf{A}}{\partial t^2} - c^2 \nabla^2 \mathbf{A} + c \nabla \frac{\partial \Phi}{\partial t} = 4\pi c \mathbf{J}, \quad (2)$$

where the Coulomb gauge,  $\nabla \cdot \mathbf{A} = 0$ , is chosen because it allows for a clear separation of the slowly and rapidly varying components of the electric field.

From here on we will use a normalized vector potential:  $\mathbf{A} \rightarrow \mathbf{A}_n \equiv e \mathbf{A} / mc^2 \equiv \sqrt{I_n}$ . To single out the rapid laser variations, we take a trial function of the form

$$\mathbf{A}_n = a_n(\mathbf{r}, t) e^{i(k_0 z - \omega_0 t - \psi(\mathbf{r}, t))} (\hat{\mathbf{x}} + i\hat{\mathbf{y}}), \quad (3)$$

where we have chosen the coordinate system so that the  $z$  axis coincides with the direction of propagation,  $a_n(\mathbf{r}, t)$  and  $\psi(\mathbf{r}, t)$  are real functions of space and time, and  $k_0$  and  $\omega_0$  are the (constant) wave number and frequency of the laser wave in uniform, unperturbed plasma. The wave is taken to have circular polarization.

Next we apply the slowly varying envelope approximation: the characteristic spatial length of the structure in our system is assumed much greater than the wavelength of the wave and the characteristic time period involved is assumed to be much longer than the laser oscillation period:

$$\begin{aligned} \left| \frac{\partial a_n}{\partial z} \right| &\ll k_0 a, \\ \left| \frac{\partial a_n}{\partial t} \right| &\ll \omega_0 a, \\ \left| \frac{\partial \psi}{\partial z} \right| &\ll k_0, \\ \left| \frac{\partial \psi}{\partial t} \right| &\ll \omega_0. \end{aligned} \quad (4)$$

The electron velocity is approximately given by

$$\mathbf{v} = \frac{\mathbf{p}}{m\gamma} = \frac{\epsilon}{mc} \frac{\mathbf{A}}{\sqrt{1+I_n}}, \quad (5)$$

and the plasma current can be written as

$$\mathbf{J} = -en_e \mathbf{v} = -\frac{\omega_p^2}{4\pi c} \frac{N_e}{\sqrt{1+I_n}} \mathbf{A}, \quad (6)$$

where  $N_e \equiv 1 + \delta n_e / n_0$  and only electrons contribute to the current. The wave equation thus becomes

$$\begin{aligned} \left[ \frac{1}{c^2} \left\{ \frac{1}{a_n} \left[ \frac{\partial^2 a_n}{\partial t^2} - 2i \left( \omega_0 + \frac{\partial \psi}{\partial t} \right) \frac{\partial a_n}{\partial t} \right] - \left( \omega_0 + \frac{\partial \psi}{\partial t} \right)^2 - i \frac{\partial^2 \psi}{\partial t^2} \right\} - \frac{1}{a_n} \left[ \nabla^2 a_n + 2ik_0 \frac{\partial a_n}{\partial z} - 2i(\nabla a_n) \cdot (\nabla \psi) \right] \right. \\ \left. + \left[ k_0 - \frac{\partial \psi}{\partial z} \right]^2 + |\nabla_T \psi|^2 + i \nabla^2 \psi \right] \mathbf{A}_n + \frac{e}{mc^3} \nabla \frac{\partial \psi}{\partial t} = -\frac{1}{\lambda_c^2} \frac{N_e}{\sqrt{1+I_n}} \mathbf{A}_n, \quad (7) \end{aligned}$$

where  $\lambda_c \equiv c / \omega_p$  is the collisionless skin depth, and  $\nabla_T$  is the transverse part of the gradient,  $\nabla = \nabla_T + (\partial / \partial z) \hat{\mathbf{z}}$ . The right-hand side of Eq. (7) represents all the relevant nonlinearities, i.e., the effect of the pondermotive force [acting through the normalized electron density  $N_e$  as will be given below by Eq. (11)] and the relativistic electron mass effects (appearing as the inverse square-root factor).

According to the slowly varying envelope approximation no significant development takes place in the time scale of the rapid laser oscillations. For this approximation to be reasonable, the plasma has to be sufficiently underdense; i.e.,  $\omega_p / \omega_0 \ll 1$ . We then average the wave equation, multiplied by the complex conjugate of the vector potential, over the laser oscillation period  $T_0 = 2\pi / \omega_0$  and arrive at the following equation that describes the slow evolution of the beam envelope:

$$\begin{aligned} \frac{1}{c^2} a_n \left[ \frac{\partial^2 a_n}{\partial t^2} - 2i \left( \omega_0 + \frac{\partial \psi}{\partial t} \right) \frac{\partial a_n}{\partial t} \right] - a_n^2 \left[ \left( \omega_0 + \frac{\partial \psi}{\partial t} \right)^2 + i \frac{\partial^2 \psi}{\partial t^2} \right] \\ - a_n \left[ \nabla^2 a_n + 2ik_0 \frac{\partial a_n}{\partial z} - 2i(\nabla a_n) \cdot (\nabla \psi) \right] + a_n^2 \left[ \left[ k_0 - \frac{\partial \psi}{\partial z} \right]^2 + |\nabla_T \psi|^2 + i \nabla^2 \psi \right] = -\frac{1}{\lambda_c^2} \frac{N_e}{(1+a_n^2)^{1/2}} a_n^2, \quad (8) \end{aligned}$$

where the scalar potential, being a slowly varying quantity, disappears in the averaging when multiplied by  $\mathbf{A}^*$ . The real terms of Eq. (8) yield an equation describing the evolution of the amplitude,

$$\frac{\partial^2 a_n}{\partial t^2} = a_n \left[ \left( \omega_0 + \frac{\partial \psi}{\partial t} \right)^2 + c^2 \nabla^2 a_n - c^2 a_n \left[ \left[ k_0 - \frac{\partial \psi}{\partial z} \right]^2 + |\nabla_T \psi|^2 \right] - \omega_p^2 \frac{N_e}{(1+a_n^2)^{1/2}} a_n \right], \quad (9)$$

while the imaginary terms of (8) yield an equation for the phase shift,

$$\frac{\partial}{\partial t} \left[ a_n^2 \frac{\partial \psi}{\partial t} \right] = -\omega_0 \frac{\partial a_n^2}{\partial t} - c^2 k_0 \frac{\partial a_n^2}{\partial z} + c^2 (\nabla a_n^2) \cdot (\nabla \psi) + c^2 a_n^2 \nabla^2 \psi. \quad (10)$$

We shall look for a stationary state, assuming that the outward laser ponderomotive force exerted on the electrons is balanced by the electrostatic field produced by the charge separation when the electrons are driven outward:

$$\mathbf{F}_p - e\mathbf{E}_0 = 0,$$

where  $\mathbf{F}_p = -mc^2 \nabla \sqrt{1+a_n^2}$  is the ponderomotive force. Taking the divergence of the force balance equation and using Gauss' law, we obtain the following expression for the electron density perturbation,

$$N_e \equiv 1 + \frac{\delta n_e}{n_0} = 1 + \lambda_c^2 \left[ \frac{1}{r} \frac{\partial}{\partial r} r \frac{\partial}{\partial r} + \frac{\partial^2}{\partial z^2} \right] \sqrt{1+I_n}, \quad (11)$$

where we have also assumed axial symmetry,  $\partial/\partial\theta=0$ . It is important to notice that this particular model does not have a mechanism for preventing negative—and thus unphysical—values for electron density. Therefore, once a solution is obtained using this model, it is necessary to check if the solution corresponds to physically meaningful values of electron density. For the stationary state described, the field equations become

$$2k_0 \frac{\partial \psi}{\partial z} - |\nabla \psi|^2 + \frac{1}{a} \nabla^2 a - \frac{1}{\lambda_c^2} \frac{N_e}{\sqrt{1+a^2}} + \left[ \frac{\omega_0^2}{c^2} - k_0^2 \right] = 0, \quad (12)$$

and

$$-k_0 \frac{\partial a^2}{\partial z} + (\nabla a^2) \cdot (\nabla \psi) + a^2 \nabla^2 \psi = 0. \quad (13)$$

Here (and henceforth) we have dropped the subscript  $n$  for convenience.

### III. ASYMPTOTIC FORM OF THE LASER PROFILE

We look for a stationary and asymptotic intensity profile independent of  $z$  for the laser beam under the combined influence of the ponderomotive and relativistic effects. We choose the following ansatz for the amplitude and phase:

$$\begin{aligned} a(r, z) &= a(r), \\ \psi(r, z) &= f(z) + g(r), \end{aligned} \quad (14)$$

where we have still allowed for phase modulation in  $z$ . Equations (12) and (13) are separable under this ansatz. Equation (12) yields

$$\begin{aligned} -2k_0 \frac{df}{dz} - \kappa_0^2 + \left[ \frac{df}{dz} \right]^2 &= C_1 \\ &= \frac{1}{a} \frac{1}{r} \frac{d}{dr} r \frac{da}{dr} \\ &\quad - \left[ \frac{dg}{dr} \right]^2 - \frac{1}{\lambda_c^2} \frac{N_e}{\sqrt{1+a^2}}, \end{aligned} \quad (15)$$

where  $\kappa_0^2 \equiv \omega_0^2/c^2 - k_0^2$ , and  $C_1$  is the separation constant. The phase equation (13) yields

$$-\frac{d^2 f}{dz^2} = C_2 = \frac{1}{r} \frac{d}{dr} r \frac{dg}{dr} + \frac{1}{a^2} \frac{da^2}{dr} \frac{dg}{dr}, \quad (16)$$

where  $C_2$  is the separation constant.

Equation (16) requires the  $z$ -dependent part of the phase shift  $\psi$  to have the form

$$f(z) = -\frac{1}{2} C_2 z^2 + C_3 z, \quad (17)$$

where the (arbitrary) constant phase shift has been dropped. Now substituting Eq. (17) into Eq. (15) implies

$$\begin{aligned} C_2 &= 0, \\ C_3 &= k_0 \pm (k_0^2 + \kappa_0^2 + C_1)^{1/2}, \end{aligned} \quad (18)$$

and thus  $f(z)$  is given by the linear expression

$$f(z) = k_0 z \pm \left[ \frac{\omega_0^2}{c^2} + C_1 \right]^{1/2} z. \quad (19)$$

The assumption of slow modulations,  $|\partial\psi/\partial z| \ll k_0$ , implies that we have to choose the square root with the negative sign to retain consistency. Thus

$$f(z) = k_0 z - \left[ \frac{\omega_0^2}{c^2} + C_1 \right]^{1/2} z, \quad (20)$$

where for consistency  $C_1$  should be much less than  $k_0^2$  in an underdense plasma. The constant  $C_1$  can be interpreted as a measure of the  $z$  dependence of the phase modulation. The radial portions of Eqs. (15) and (16) can now be written as

$$\begin{aligned} \frac{1}{a} \frac{1}{r} \frac{d}{dr} r \frac{da}{dr} - \left[ \frac{dg}{dr} \right]^2 - \frac{1}{\lambda_c^2} \frac{N_e}{(1+a^2)^{1/2}} &= C_1, \\ \frac{1}{r} \frac{d}{dr} r \frac{dg}{dr} + \frac{1}{a^2} \frac{da^2}{dr} \frac{dg}{dr} &= 0. \end{aligned} \quad (21)$$

#### A. Slab approximation

Equations (21) in the slab limit are

$$\frac{1}{a} \frac{d^2}{dx^2} a - \left[ \frac{dg}{dx} \right]^2 - \frac{1}{\lambda_c^2} \frac{N_e}{(1+a^2)^{1/2}} = C_1, \quad (22)$$

and

$$a^2 \frac{dg}{dx} = C_4, \quad (23)$$

where the phase equation was integrated once over  $x$ , bringing about the integration coefficient  $C_4$ , which can

be interpreted to be a measure of the amplitude dependent transverse phase modulation. Combining Eqs. (22) and (23) yields a differential equation for  $a$  only:

$$\frac{1}{a} \frac{d^2}{dx^2} a - \frac{C_4^2}{a^4} - \frac{1}{\lambda_c^2} \frac{N_e}{(1+a^2)^{1/2}} = C_1, \quad (24)$$

with

$$N_e = 1 + \lambda_c^2 \frac{d^2}{dx^2} (1+a^2)^{1/2}. \quad (25)$$

Using Eq. (25), the amplitude equation becomes

$$\begin{aligned} \frac{1}{a} \frac{d^2}{dx^2} a - \frac{C_4^2}{a^4} - \frac{1}{\lambda_c^2} \frac{1}{(1+a^2)^{1/2}} \\ = \frac{1}{(1+a^2)^{1/2}} \frac{d^2}{dx^2} (1+a^2)^{1/2} = C_1. \end{aligned} \quad (26)$$

An equation of the form of Eq. (26) can be derived from Hamilton's principle. Treating Eq. (26) as the "equation of motion" for the laser-plasma system with the coordinate  $x$  playing the role of time, we write the Lagrangian of the system in the form

$$L = g(a) \frac{(a')^2}{2} - V(a), \quad (27)$$

where  $g(a)$  is a metric and  $V(a)$  is the potential of the system, both yet to be determined, and where prime stands for the derivative with respect to the timelike variable. Lagrange's equation then yields

$$g(a)a'' + \frac{1}{2} \frac{dg}{da} (a')^2 + \frac{\partial V}{\partial a} = 0. \quad (28)$$

We find an integrating factor  $\mu(a)$  by requiring that Eq. (26) multiplied by  $\mu(a)$  should coincide with Eq. (28). We thus obtain

$$\begin{aligned} \mu(a) &= a, \\ g(a) &= \frac{1}{1+a^2}, \end{aligned} \quad (29)$$

and from Eq. (26) the potential is seen to be

$$V(a) = \frac{1}{2} \frac{C_4^2}{a^2} - \frac{1}{\lambda_c^2} (1+a^2)^{1/2} = \frac{1}{2} C_1 a^2. \quad (30)$$

Applying Noether's theorem we can now write down the first integral of Eq. (26),

$$\begin{aligned} \mathcal{E} &= \frac{\partial L}{\partial a'} a' - L(a, a') \\ &= \frac{1}{2} g(a) (a')^2 + V(a). \end{aligned} \quad (31)$$

Thus,

$$\mathcal{E} = \frac{(a')^2}{2(1+a^2)} + \frac{C_4^2}{2a^2} - \frac{1}{\lambda_c^2} (1+a^2)^{1/2} - \frac{C_1}{2} a^2. \quad (32)$$

### B. Potential analysis

We shall now classify the possible solutions to Eq. (26). However, since the system has a nontrivial metric, the in-

terpretation of the potential as given by Eq. (30) is difficult. Therefore, we find a point transformation that will flatten the metric. Writing the coordinate  $a$  as a function of a new variable  $y$ ,  $a = f(y)$ , we require that  $\partial f / \partial y \neq 0$  for all values of  $y$  so that the mapping is one to one. In terms of the new variable the Lagrangian of the system becomes

$$L(y, y') = \frac{1}{2} \frac{\partial f}{\partial y} (1+f^2)^{-2} (y')^2 - V(f(y)). \quad (33)$$

We arrive at a coordinate system with a flat metric by requiring that

$$\frac{\partial f}{\partial y} \frac{1}{(1+f^2)^2} = 1, \quad (34)$$

which, upon integration yields

$$f(y) = \sinh(y), \quad (35)$$

where the integration constant has been chosen such that the origin of  $a$  and  $y$  are aligned.

Introducing the change of variable according to  $a = \sinh y$  and using a dimensionless transverse coordinate  $\xi \equiv x / \lambda_c$ , Eq. (32) becomes

$$\frac{1}{2} \left[ \frac{dy}{d\xi} \right]^2 + V(y) = \mathcal{E}, \quad (36)$$

where  $\mathcal{E}$  is the "total energy" of the system, and

$$V(y) = \frac{\bar{C}_4^2}{2 \sinh^2 y} - \cosh y - \frac{\bar{C}_1}{2} \sinh^2 y \quad (37)$$

is the "potential" describing the behavior of the system. The bars above the integration constants indicate the factor of  $\lambda_c^2$  brought in by the normalization of the variable  $x$ :  $\bar{C}_1 = C_1 \lambda_c^2$ , and  $\bar{C}_4 = C_4 \lambda_c$ .

The qualitative nature of the solutions can be studied by finding the possible "humps" of the potential. Setting the first derivative of the potential equal to zero, the location of the humps is given by

$$2\bar{C}_4 X + (X^2 - 1)^2 (1 + 2\bar{C}_1 X) = 0, \quad (38)$$

where  $X \equiv \cosh y \geq 1$ . We study this for different values of the constants  $\bar{C}_1$  and  $\bar{C}_4$ .

#### 1. $\bar{C}_4 = 0$

The possible roots are  $X = 1$  and  $X = -1/2\bar{C}_1$  corresponding to  $y = 0$  and  $y = \text{arcosh}(-1/\bar{C}_1)$ . Since  $X$  is restricted by  $X \geq 1$ , the second root exists only for  $-1 < \bar{C}_1 < 0$ . The potential for these cases is sketched in Fig. 1(a) (solid line). For  $-1 < \bar{C}_1 < 0$  a homoclinic orbit as well as oscillating solutions (depending on the value of  $\mathcal{E}$ ) are possible. For  $\bar{C}_1 > 0$  there are no bound solutions as indicated by the form of the potential in Fig. 1(b). Figure 1(c) shows the potential for  $\bar{C}_1 < -1$ . Since the amplitude is not allowed to have negative values, this potential does not correspond to conventional oscillations. To make a clear distinction, we shall call the conventional oscillations introduced by the potential of Fig. 1(a) type-I oscillations, whereas the oscillations exhibited by the po-

tential of Fig. 1(c) will be called type-II oscillations. The type-II oscillations corresponding to this parameter regime will be discussed in more detail below.

It should be noted that although in our slab approxi-

mation the total power associated with the oscillating solutions is infinite, these solutions cannot be dismissed as unphysical, as the relevant quantity is the total power per unit length (e.g., the wavelength of one oscillation).

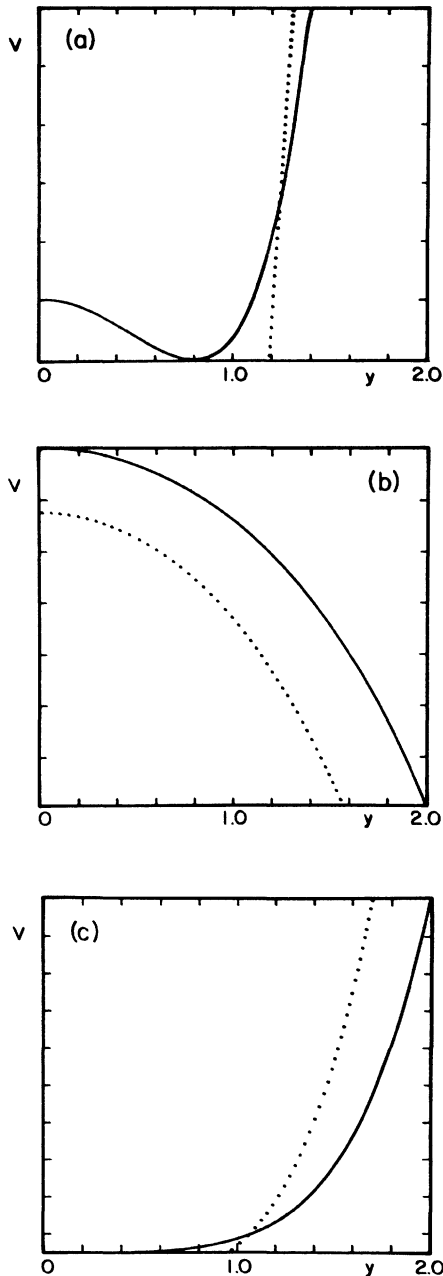


FIG. 1. (a) The characteristic potential  $V(y)$  (solid curve) of the laser-plasma system for  $\bar{C}_4^2=0$ ,  $-1 < \bar{C}_1 < 0$ , and the density depletion curve (dotted curve). (b) The characteristic potential  $V(y)$  (solid curve) of the laser-plasma system for  $\bar{C}_4^2=0$ ,  $\bar{C}_1 > 0$ , and the density depletion curve (dotted curve). (c) The characteristic potential  $V(y)$  (solid curve) of the laser-plasma system for  $\bar{C}_4^2=0$ ,  $\bar{C}_1 < -1$ , and the density depletion curve (dotted curve).

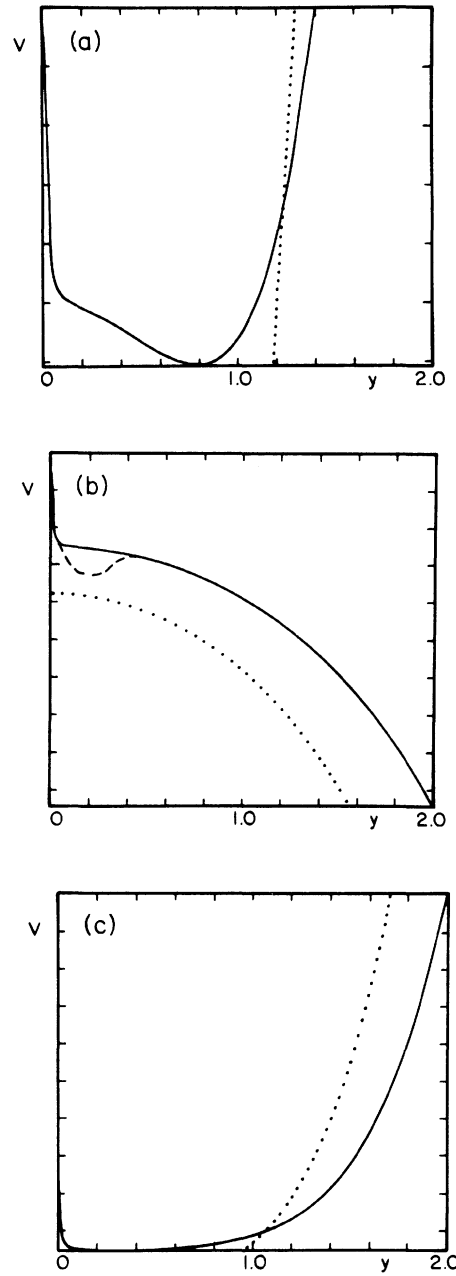


FIG. 2. (a) The characteristic potential  $V(y)$  (solid curve) of the laser-plasma system for  $\bar{C}_4^2=0$ ,  $-1 < \bar{C}_1 < 0$ , and the density depletion curve (dotted curve). (b) The characteristic potential  $V(y)$  (solid curve) of the laser-plasma system for  $\bar{C}_4^2 \neq 0$ ,  $\bar{C}_1 > 0$ , and the density depletion curve (dotted curve). (c) The characteristic potential  $V(y)$  (solid curve) of the laser-plasma system for  $\bar{C}_4^2 \neq 0$ ,  $\bar{C}_1 < -1$ , and the density depletion curve (dotted curve).

2.  $\bar{C}_4^2 > 0$

Assume  $|\bar{C}_4| \ll 1$ , for otherwise vanishingly small values of the amplitude would dominate the behavior of the system. The extremum at  $y=0$  found for  $\bar{C}_4=0$  is now replaced by a divergence,  $V(y=0) \rightarrow +\infty$ . The form of the potential for  $-1 < \bar{C}_1 < 0$  is plotted in Fig. 2(a). The homoclinic orbit has disappeared and only the oscillating solutions survive. For  $\bar{C}_1 > 0$  the potential is plotted in Fig. 2(b). In principle the system could now have bound solutions for these values of  $\bar{C}_1$  as indicated by the dashed curve. This does not, however, seem to be the case. Since  $|\bar{C}_4| \ll 1$  and  $X=1$  is a root for  $\bar{C}_4=0$ , we try to find the possible extrema necessary for bound solutions in the form  $X=1+\delta$ ,  $0 < \delta \ll 1$ . Substituting this ansatz into Eq. (38) we obtain, keeping terms up to the second order in  $\delta$ ,

$$\delta = \frac{1}{2(1+2\bar{C}_1)} \{ -\bar{C}_4 \pm [\bar{C}_4^2 - 8\bar{C}_4(1+2\bar{C}_1)]^{1/2} \}. \quad (39)$$

But for  $\bar{C}_1, \bar{C}_4 > 0$ , and  $|\bar{C}_4| \ll 1$  the term in curly brackets becomes a complex quantity, and thus the potential does not have this type of a root. Therefore the system seems to still lack bound solutions for these values of  $\bar{C}_1$ . Figure 2(c) shows the potential for  $\bar{C}_1 < -1$ . The presence of type-II oscillations is now clear due to the wall that has appeared at the origin.

In Fig. 3 we have sketched the different possible solutions. Figure 3(a) shows the solution corresponding to the homoclinic orbit, and Fig. 3(b) shows type-I oscillating solutions. Since  $\bar{C}_4=0$ , the phase is constant in the transverse direction in both cases. In Fig. 3(c) we show the type-II oscillations together with the nontrivial phase profile in the transverse direction. The solutions corresponding to the potential of Fig. 1(c) (dashed line) are seen to be an extreme case of the type-II oscillations in which the phase becomes discontinuous and the amplitude exhibits a cycloid-type pattern.

As mentioned when introducing the model for electron density, Eq. (11), it is necessary to check if these solutions correspond to physically meaningful values of electron density. From Eq. (11) the electron density perturbation  $\delta n_e/n_0$  can be rewritten in terms of the variable  $y(\xi)$  as

$$\frac{\delta n_e}{n_0} = y'' \sinh y + (y')^2 \cosh y. \quad (40)$$

From the Hamiltonian formalism the  $y$  derivatives can be expressed in terms of the potential  $V(y)$  and the total energy of the system  $\mathcal{E}$  as

$$y'' = -\frac{\partial V}{\partial y}, \quad (41)$$

$$y' = 2(\mathcal{E} - V),$$

yielding

$$\frac{\delta n_e}{n_0} = 2\mathcal{E} \cosh y + 2\bar{C}_1 \sinh^2 y \cosh y + \sinh^2 y + 2 \cosh^2 y, \quad (42)$$

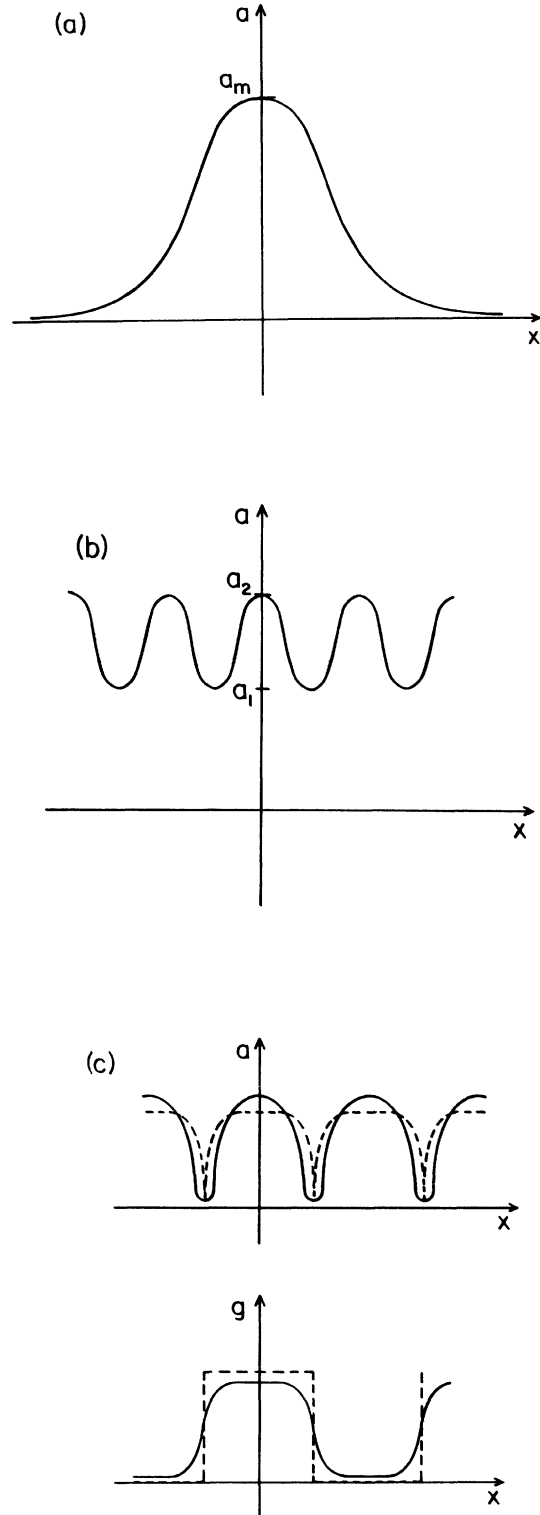


FIG. 3. (a) Solitary profile corresponding to the homoclinic orbit. (b) Multiple beamlet profile type solutions corresponding to type-I oscillatory orbits. (c) Multiple beamlet profile type solutions corresponding to type-II oscillatory orbits.

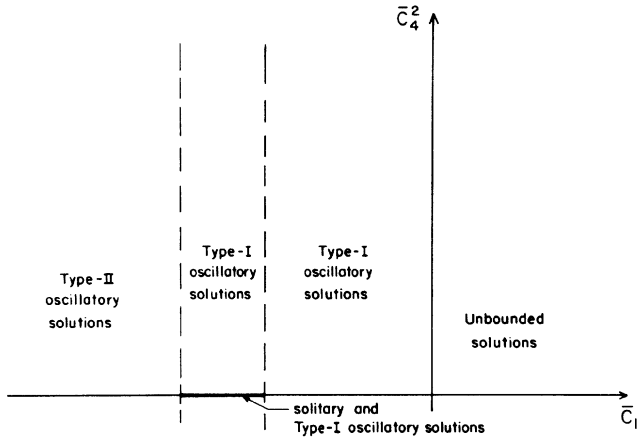


FIG. 4. The parameter space  $(\bar{C}_1, \bar{C}_4)$  with the appropriate solutions listed in each region.

an equation independent of  $\bar{C}_4$ . The critical case, corresponding to a total depletion of the electrons, is given by  $\delta n_e/n_0 = -1$ . This case is specified by the electron depletion curve given by Eq. (42) evaluated at  $\delta n_e/n_0 = -1$ :

$$\mathcal{E}(\bar{C}_1, y) = -\frac{3}{2} \cosh y - \bar{C}_1 \sinh^2 y. \quad (43)$$

The electron depletion curves as given by Eq. (43) are plotted in Figs. 1 and 2 on top of the potential curves (dotted curves). The physically meaningful solutions lie above the electron depletion curve corresponding to positive values of the electron density.

We conclude that bound physical solutions come in only two kinds. One is a solitary-wave solution, corresponding to the homoclinic orbit, the other is a multiple beamlet type, which corresponds to the type-I and type-II oscillatory solutions. The existence of these solutions is summarized in Fig. 4.

### C. Exact solutions

Seeking analytical solutions of Eq. (32) with finite total power we impose the boundary conditions:  $a, a' \rightarrow 0$  as  $x \rightarrow \infty$ . This requires that the energy  $\mathcal{E}$  and the coefficient  $C_4$  have the following values:

$$\begin{aligned} C_4 &\equiv 0, \\ \mathcal{E} &\equiv -1/\lambda_c^2. \end{aligned} \quad (44)$$

Recalling the classification of the solutions done above, this implies that we are looking for a solitary type profile sketched in Fig. 1(c). The amplitude equation now becomes

$$\begin{aligned} (a')^2 &= C_1 a^4 + \left[ C_1 - \frac{2}{\lambda_c^2} \right] a^2 - \frac{2}{\lambda_c^2} \\ &+ \frac{2}{\lambda_c^2} (1+a^2)^{3/2}. \end{aligned} \quad (45)$$

If we let  $\xi = x/\lambda_c$  (as before) and change variables according to

$$[y(\xi)]^2 = \{[a(\xi)]^2 + 1\}^{1/2} - 1,$$

Eq. (45) takes on an elementary form, which has the solution

$$y = \frac{\pm 16\kappa^2 E}{E^2 \mp 4E(2\kappa^2 - 1) + 4}, \quad (46)$$

where  $E \equiv \exp[-2\kappa(\xi + C_8)]$  and  $\kappa^2 \equiv \lambda_c^2 C_1 + 1$ . Unraveling the change of variable leads to

$$I = a^2 = \frac{\pm 32(E \pm 2)^2 \kappa^2 E}{[(E \pm 2)^2 \mp 8\kappa^2 E]^2}. \quad (47)$$

Since the intensity is positive, the upper sign in the expression (47) is relevant. The integration constant  $C_8$  embedded within  $E$  corresponds to merely a shift of the solution along the  $x$  axis. From Eq. (47) the profile centered at  $\xi = 0$  is

$$a = \frac{2\kappa \operatorname{sech}(\kappa\xi)}{1 - \kappa^2 \operatorname{sech}^2(\kappa\xi)}. \quad (48)$$

The parameter  $\kappa$  is now seen to be related to the inverse width of the profile in units of  $\lambda_c^{-1}$ . Furthermore,  $\kappa$  is directly related to both the peak intensity of the profile at  $\xi = 0$ , and to the total power of the beam:

$$a_m = a(\xi = 0) = \frac{2\kappa}{1 - \kappa^2}. \quad (49)$$

The total power of the laser beam in dimensionless variables is given by

$$\begin{aligned} P &\equiv \int_{-\infty}^{+\infty} I(\xi) d\xi \\ &= 4 \left[ \frac{\kappa}{1 - \kappa^2} + \frac{\arctan(\kappa/\sqrt{1 - \kappa^2})}{(1 - \kappa^2)^{3/2}} \right]. \end{aligned} \quad (50)$$

Equation (50) is a scaling relation between the width and the power of the laser profile. The presence of a relation between the amplitude and the width is typical of solitonlike structures, although the relation (49) is not linear and is thus different from the Korteweg-de Vries (KdV) soliton.

The condition that was obtained for the existence of bound solutions while doing the classification of the solutions,  $-1 < \bar{C}_1 < 0$ , translates into a physically reasonable condition for  $\kappa^2$ :

$$0 < \kappa^2 < 1. \quad (51)$$

The lower limit excludes trivial solutions with zero amplitudes, and the upper limit keeps the peak amplitude finite. In Fig. 5(a) we have plotted profiles for various values of maximum amplitude  $a_m$ . In Fig. 5(b) are the corresponding potentials.

Another restriction on the possible values of  $\kappa^2$  can be found by requiring that the solution correspond to physical values of the electron density given by Eq. (11). The critical case for the homoclinic orbit corresponds to the situation when the intersection of the depletion curve and the potential takes place at the maximum amplitude of the homoclinic orbit. Setting the potential given by Eq. (37) equal to the depletion curve given by Eq. (43) we obtain

$$\text{coshy}^* + \bar{C}_1 \sinh^2 y^* = 0. \quad (52)$$

For the homoclinic orbit the energy is, according to Eq. (44),  $\mathcal{E} = -1/\lambda_c^2$ . Equation (43) yields

$$\text{coshy}^* = 2. \quad (53)$$

Substituting this value for  $y^*$  back to Eq. (52) we obtain

$$\bar{C}_1 = -\frac{2}{3} \text{ or equivalently } \kappa^2 < \frac{1}{3}. \quad (54)$$

For values satisfying the condition (54), the potential lies

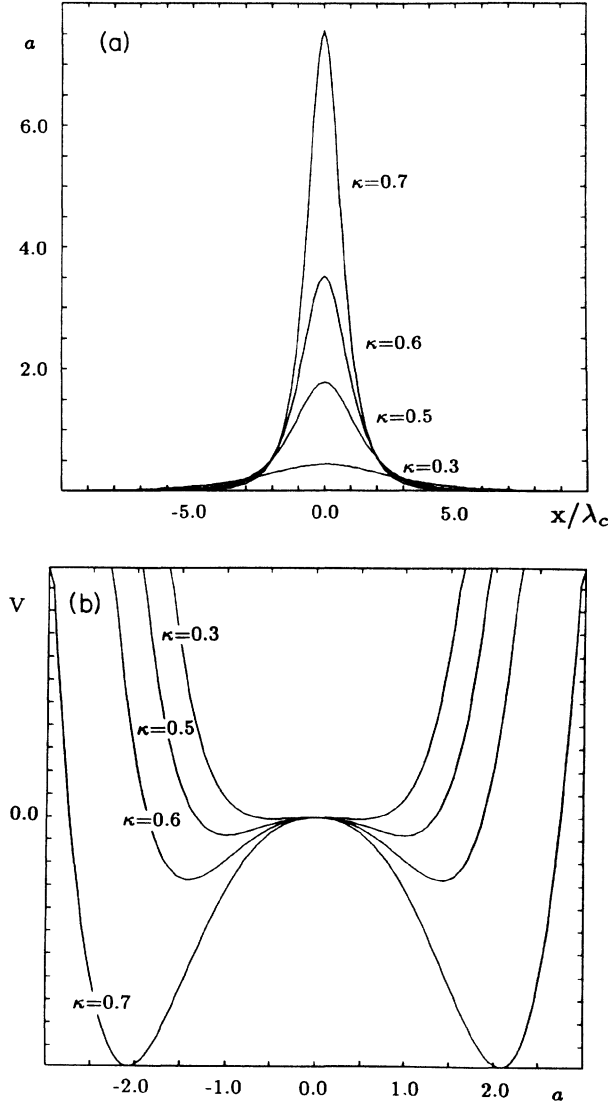


FIG. 5. (a) The asymptotic intensity profile for various values of the beam width parameter  $\kappa$ . The normalized peak amplitude,  $a_0 \equiv eE_0/mc\omega_0$ , is then given by  $I_0 = 2\kappa/1 - \kappa^2$ : (1)  $\kappa=0.3$ ,  $a_0=0.66$ , (2)  $\kappa=0.5$ ,  $a_0=1.33$ , (3)  $\kappa=0.6$ ,  $a_0=1.88$ , (4)  $\kappa=0.7$ ,  $a_0=2.75$ . (b) The characteristic potential of the system  $V(a)$  describing the beam profile plotted for the same values of  $\kappa$  as in (a).

above the depletion curve corresponding to physically meaningful values of electron density. Therefore, within the framework of the model for electron density as given by Eq. (11), the self-consistent solitary profiles are given by Eq. (48) while the width of the profile is restricted by

$$0 < \kappa^2 < \frac{1}{3}. \quad (55)$$

### 1. Nonrelativistic solutions

It is interesting to compare the results yielded by the present approach to work done earlier on the subject.<sup>9-12</sup> Schmidt and Horton<sup>12</sup> studied purely relativistic self-focusing for nonrelativistic field amplitudes,  $a^2 < 1$ . Integrating Eq. (24) once, keeping the electron density constant ( $N_e \equiv 1$ ), and expanding for  $a^2 < 1$  we obtain

$$(a')^2 = \left[ C_1 + \frac{1}{\lambda_c^2} \right] a^2 - \frac{1}{4} \frac{1}{\lambda_c^2} a^4 + O(a^6). \quad (56)$$

Recalling the shorthand notation  $\kappa^2 \equiv \lambda_c^2 C_1 + 1$ , Eq. (45) reduces to

$$\frac{d}{d\xi} a = \pm (\kappa^2 a^2 - \frac{1}{4} a^4)^{1/2}, \quad (57)$$

which yields the following expression for the intensity:

$$I(x) = -16\kappa^2 \frac{C_6 e^{\pm 2\kappa\xi}}{(1 - C_6 e^{\pm 2\kappa\xi})^2}. \quad (58)$$

For the solution to remain finite for all values of  $\xi$ ,  $C_6 \equiv -C_7 < 0$ . The profile is found to have one (and only one) extremum when  $C_7 > 0$ , a condition that coincides with the one already established above for the finiteness of the solution. The extremum,  $x_m$ , is given by

$$x_m = -\frac{\ln C_7}{2\kappa}, \quad (59)$$

and the intensity profile centered at  $\xi = 0$  is

$$I(\xi) = 4\kappa^2 \frac{1}{\cosh^2(\kappa\xi)}. \quad (60)$$

The complete solution obtained by Schmidt and Horton<sup>12</sup> is

$$I(\xi) \equiv A_n^2(\xi) = I_0 \frac{1}{\cosh^2(\sqrt{\alpha_{SH}} \xi)}, \quad \alpha_{SH} = \frac{1}{2} I_0$$

$$\varphi = (1/c) [\omega^2 + (\omega_p)^2 (\frac{1}{2} I_0 - 1)]^{1/2} z - \omega t, \quad (61)$$

while the complete solution obtained by us is

$$I(\xi) = I_0 \frac{1}{\cosh^2(\kappa\xi)}, \quad \kappa^2 = \frac{1}{4} I_0$$

$$\varphi(\xi) = (1/c) [\omega_0^2 + (\omega_p)^2 (\frac{1}{4} I_0 - 1)]^{1/2} z - \omega_0 t. \quad (62)$$

For a given frequency  $\omega = \omega_0$ , our solution coincides (within a factor of 2) with the one obtained by Schmidt and Horton. The factor of 2 difference arises from the different choice for the polarization of the laser field: Schmidt and Horton assumed a linearly polarized wave for which the time averaging process produces a factor of



$\frac{1}{2}$ , whereas in this work we have used circular polarization for which the time averaging does not introduce any numerical factors. Taking this difference into account, it is seen that the profiles are consistent.

#### IV. NUMERICAL RESULTS

In this section we compare the theoretical results derived in the preceding sections with a recently developed computer simulation.<sup>13</sup> The reason for this is twofold.

On the one hand, exact results are useful as test cases for verifying the correctness of a computer code, and on the other hand, computer codes can give evidence for stability of solutions. Although the solutions we have presented here are exact, their occurrence depends critically upon stability. In general, proving stability of solitonlike solutions is a difficult task, so the computer is a useful tool in this respect.

The code used is a time averaged particle simulation code developed for modeling transport of optical beams

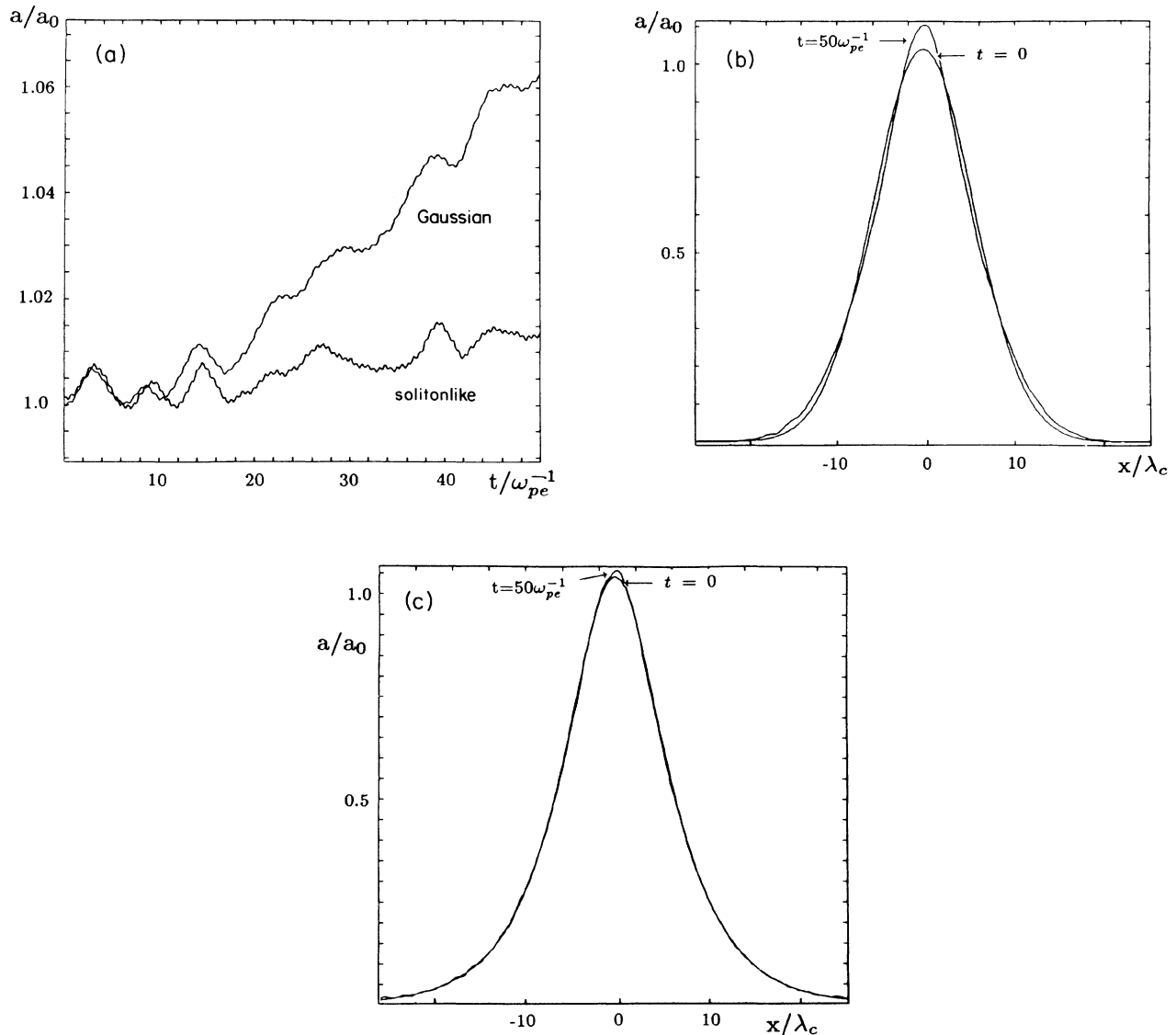


FIG. 6. (a) The peak amplitude of the different profiles as a function of time. The vertical axis gives the ratio of the observed amplitude  $a$  to the original amplitude  $a_0$ . The Gaussian beam self-focuses as indicated by the rapidly growing amplitude, whereas the solitonlike profile propagates practically unaltered. The time is expressed in the units of  $\omega_p^{-1}$ . (b) The beam profile of an originally Gaussian beam plotted at  $t=0$  and  $50\omega_p^{-1}$ . The form of the profile gets severed. (c) The beam profile of a solitonlike beam plotted at  $t=0$  and  $50\omega_p^{-1}$ . The beam is seen to retain its shape.

in plasmas.<sup>13</sup> The code operates on the same principles as any standard electromagnetic particle simulation code, except that it uses the wave equation, which is phase averaged over the rapid laser oscillations. Similarly, the equation of motion for the relativistic electrons is averaged, thus yielding the laser contribution in the form of the ponderomotive force. We have here used a version of the code that is formally one dimensional but which in fact portrays a two-dimensional situation—the code “time” representing the direction of propagation for a stationary state. The code uses periodic boundary conditions, the width of the simulation box is chosen to be  $51.2\lambda_c$  and there are 100 electrons per grid cell. The number of grid points for the simulations discussed below was 256 and the time step was chosen at  $dt = 0.1\omega_p^{-1}$ .

In the first case we set up a Gaussian intensity profile with normalized intensity (quivering velocity)  $I = 0.16$  and beam waist  $w_b = 8\lambda_c$ , and the laser frequency was chosen to be  $\omega_0 = 5\omega_p$ , although  $\omega_0$  can be much greater than this choice without an increase of cost in our code. For these parameters the beam should self-focus (see Refs. 8 and 9), and it is indeed observed to focus as indicated by the increasing peak amplitude in Fig. 6(a). We then replace the Gaussian intensity profile by the  $\text{sech}^2$  profile derived above for the asymptotic profile. The profile should then remain practically unaltered while propagating in plasma, as it is a steady-state solution. This turns out to be the case, as evidenced in Fig. 6(a), which shows that the fluctuations in the peak amplitude do remain within 1%. Also, the form the beam retains its  $\text{sech}^2$  profile, whereas in the case of the Gaussian profile quite strong deviation from the original form is

observed [see Figs. 6(b) and 6(c)]. Thus we conclude that the  $\text{sech}^2$  profile is a realistic physical candidate for the asymptotic shape of a self-focused laser beam.

## V. DISCUSSION

We have addressed here the question of a possible asymptotic transverse profile for a short, self-focused laser pulse propagating in plasma. Using a stationary-state model for the electron density, we arrived at a solitary wave shape and a multiple beamlet shape for the asymptotic profile. In the nonrelativistic limit for the field intensity, keeping only relativistic electron effects, the result reduces to the one obtained earlier by Schmidt and Horton.<sup>12</sup> The general profile (including ponderomotive effects) agrees well with computation proving to be stable and stationary in the numerical particle simulation experiment.

The existence of a stable asymptotic profile of a self-focused laser beam may have important applications in, e.g., laser fusion as well as in plasma based accelerators, where it is necessary to have the laser beam traverse considerable distances without significant depletion.

## ACKNOWLEDGMENTS

Two of us (T.K.S. and T.T.) would like to thank Professor Huson for his encouragement. This work was supported by the U.S. Department of Energy Contract Nos. DE-AC02-87ER-40338 and DE-FG05-80ET-53088, National Science Foundation Grant No. ATM-85-06646, and HARC Grant No. 88-T55-1.

<sup>1</sup>S. A. Akhmanov, A. P. Sukhurov, and R. V. Khokhlov, *Sov. Phys.—Usp.* **10**, 609 (1968).

<sup>2</sup>T. Tajima and J. M. Dawson, *Phys. Rev. Lett.* **43**, 267 (1979).

<sup>3</sup>T. Tajima, in *Proc. 12th International Conference High Energy Accelerators*, edited by F. T. Cole and R. Donaldson (Fermi National Accelerator Laboratory, Batavia, Illinois, 1983).

<sup>4</sup>Y. Kodama and A. Hasegawa, *Opt. Lett.* **8**, 342 (1983).

<sup>5</sup>K. Ohkuma, Y. H. Ichikawa, and Y. Abe, *Opt. Lett.* **12**, 516 (1987).

<sup>6</sup>K. Mima, T. Ohsuga, H. Takabe, K. Nishihara, T. Tajima, E. Zaidman, and W. Horton, *Phys. Rev. Lett.* **57**, 1421 (1986).

<sup>7</sup>F. S. Felber, *Phys. Fluids* **23**, 1411 (1980).

<sup>8</sup>F. W. Perkins and E. J. Valeo, *Phys. Rev. Lett.* **32**, 1234 (1974).

<sup>9</sup>D. C. Barnes, T. Kurki-Suonio, and T. Tajima, *IEEE Trans. Plasma Science* **PS-15**, 154 (1987).

<sup>10</sup>G.-Z. Sun, E. Ott, Y. C. Lee, and P. Guzdar, *Phys. Fluids* **30**, 526 (1987).

<sup>11</sup>P. Sprangle, C.-M. Tang, and E. Esarey, *IEEE Trans. Plasma Science* **PS-15**, 145 (1987).

<sup>12</sup>G. Schmidt and W. Horton, *Commun. Plasma Phys. Controlled Fusion* **E 9**, 85 (1985).

<sup>13</sup>T. Kurki-Suonio and T. Tajima (unpublished).